Cancer Biology & Therapy 12:9, 818-826; November 1, 2011; © 2011 Landes Bioscience

VMY-1-103 is a novel CDK inhibitor that disrupts chromosome organization and delays metaphase progression in medulloblastoma cells

Lymor Ringer,[1] Paul Sirajuddin,[1] Mary Heckler,[1] Anup Ghosh,[1] Frank Suprynowicz,[2] Venkata M. Yenugonda,[3] Milton L. Brown,[1,3] Jeffrey A. Toretsky,[1] Aykut Uren,[1] YiChien Lee,[1] Tobey J. MacDonald,[4] Olga Rodriguez,[1] Robert I. Glazer,[1] Richard Schlegel[1,2] and Chris Albanese[1,2,*]

[1]Lombardi Comprehensive Cancer Center and Department of Oncology; [2]Department of Pathology; [3]Drug Discovery Program; Georgetown University Medical Center; Washington DC; [4]Department of Pediatrics; Emory University School of Medicine; Atlanta, GA USA

Keywords: medulloblastoma, apoptosis, mitotic catastrophe, CDK inhibitor, mitosis, cell cycle

Medulloblastoma is the most prevalent of childhood brain malignancies, constituting 25% of childhood brain tumors. Craniospinal radiotherapy is a standard of care, followed by a 12 mo regimen of multi-agent chemotherapy. For children less than 3 y of age, irradiation is avoided due to its destructive effects on the developing nervous system. Long-term prognosis is worst for these youngest children and more effective treatment strategies with a better therapeutic index are needed. VMY-1-103, a novel dansylated analog of purvalanol B, was previously shown to inhibit cell cycle progression and proliferation in prostate and breast cancer cells more effectively than purvalanol B. In the current study, we have identified new mechanisms of action by which VMY-1-103 affected cellular proliferation in medulloblastoma cells. VMY-1-103, but not purvalanol B, significantly decreased the proportion of cells in S phase and increased the proportion of cells in G_2/M. VMY-1-103 increased the sub G_1 fraction of apoptotic cells, induced PARP and caspase-3 cleavage and increased the levels of the Death Receptors DR4 and DR5, Bax and Bad while decreasing the number of viable cells, all supporting apoptosis as a mechanism of cell death. $p21^{CIP1/WAF1}$ levels were greatly suppressed. Importantly, we found that while both VMY and flavopiridol inhibited intracellular CDK1 catalytic activity, VMY-1-103 was unique in its ability to severely disrupt the mitotic spindle apparatus, significantly delaying metaphase and disrupting mitosis. Our data suggest that VMY-1-103 possesses unique antiproliferative capabilities and that this compound may form the basis of a new candidate drug to treat medulloblastoma.

Introduction

During brain development and maturation, and in anticipation of populating the cerebral cortex with granular neurons, a burst of postnatal granular neuronal precursor cell proliferation occurs in the external granular layer of the brain. Following this period of rapid precursor cell expansion, an orderly exit from the cell cycle and coordinated migration and differentiation is required to direct the proper formation of the granular layer of the cerebellum, and a failure of normal differentiation and migration of the granular precursor cells is believed to be the cellular basis for a majority of medulloblastomas (MB) (reviewed in ref. 1). While locally advanced MB can have profound effects per se, one of the underlying clinical challenges related to MB treatment is its proclivity to spread throughout the neuraxis. Therefore, craniospinal radiotherapy is a standard of care delivered to children immediately after surgical resection of the tumor, followed by a 12 mo regimen of intensive multi-agent chemotherapy. While effective, this course of treatment has serious consequences. For example, a majority of survivors are left with auditory and growth deficits, and recent studies have demonstrated that irradiation significantly lowers cognitive development and function in 9 of the 12 intelligence subtest categories studied (reviewed in ref. 2). Irradiation is therefore avoided in children less than three years old due to its destructive effects on the developing nervous system. Long-term prognosis for these children is considerably worse and significant effort is underway to develop more effective MB treatment strategies.[3]

The etiology of MB is complex, and the heterogeneity of the tumors that arise is partially understood via identified alterations in genes and signaling pathways that either direct cell expansion or inhibit proliferation. Clinically, MBs have been assigned to five pathologically defined subtypes, and molecular profiling has further subclassified the tumors based on gene expression patterns and chromosomal abnormalities.[4-6] Dysregulation of Hedgehog (Hh) signaling, defined as the c3 MB subgroup,[6] is the most frequent developmental signaling pathway alteration in MBs, being found at the highest frequency in both children under 3 y of age

*Correspondence to: Chris Albanese; Email: albanese@georgetown.edu
Submitted: 07/28/11; Revised: 08/06/11; Accepted: 08/09/11
DOI: 10.4161/cbt.12.9.17682

and in all MB patients over the age of 25.[6] Hh-associated MB tumors contain changes in the abundance of multiple proteins involved in cell cycle regulation, including Gli, cyclins D1 and D2 as well as N-Myc.[7] Similarly, a Myc activation signature is a defining characteristic of the c1 subgroup, and this group shows the worst overall survival, followed by the c3/Hh subgroup. The human MB cell lines, DAOY and D556 resemble the c3 and c1 subgroup, respectively, as maintenance of activated Smo signaling[8] and Gli transactivation[9] is required for DAOY cell proliferation, while D556 cells have amplified Myc.[10]

Regardless of the underlying cause, the tumors that form are highly proliferative, and more effective clinical treatments will require developing therapies that target critical components of the cell proliferation machinery.

The cyclins are regulatory proteins that modulate the activity of the cyclin-dependent kinases (Cdks), thereby directing the orderly progression of eukaryotic cells through the cell cycle.[11] Because of the prominent loss of normal cell cycle control and due to the extensive proliferation that is associated with MB, we anticipate that the ability to treat MB may be enhanced through identifying small molecule inhibitors that target critical components of the cell cycle regulatory machinery.[9] The 2,6,9-trisubstituted purine group of cyclin dependent kinase inhibitors act by competing with ATP in targeted CDK's.[12] We have recently developed a novel purvalanol B (PVB)-based small molecule inhibitor termed VMY-1-103 (VMY). This compound was synthesized with 6-anilino position coupling of a dansyl ethylenediamine group to both retain CDK-inhibitory function and enable fluorescent imaging capability.[13,14] We established that VMY exhibited a significant increase in potency vs. PVB in inducing cell cycle arrest and apoptosis in human prostate and breast cancer cell lines while still remaining largely inactive in immortalized cells, consistent with this group of inhibitors.[13,14] We believe that the increased potency of VMY may be due in part to the lipophilic dansyl side-group supporting increased cell membrane permeability. In the present study using human medulloblastoma cell lines, we present data that further establishes that VMY exhibits increased potency at inducing G_2/M arrest and in inducing apoptosis, PARP- and caspase-3-cleavage and increasing the levels of DR4, DR5, Bax and Bad vs. its parent compound, PVB. Importantly, we also present new findings demonstrating that while VMY was as effective as flavopiridol at inhibiting intracellular CDK1 enzymatic activity, achieving a greater than 90% inhibition, only VMY disturbed centrosome polarity, affecting chromosomal alignment and migration, thereby significantly disrupting mitosis. Our results indicate that VMY has unique properties related to its ability to rapidly disrupt the mitotic apparatus, potentially differentiating VMY from other small molecule CDK inhibitors.

Results

VMY inhibits cell cycle progression in DAOY. We have recently described the effects of VMY, a novel dansylated-analog of purvalanol B on prostate and breast cancer cell lines.[13,14] In the present study, DAOY and D556 human medulloblastoma cell lines were utilized to assess the effect of VMY on MB cell cycle progression. DAOY cells were treated for 18 h with purvalanol B (PVB) or VMY at varying concentrations, or LY294002 at 20 uM as a control for cell cycle arrest (**Fig. 1A**). Treatment with LY294002 resulted in an increase in the number of cells in G_1 and a concomitant decrease in the number of cells in S-phase. PVB had no significant effect (**Fig. 1A**). Conversely, VMY significantly affected a G_2/M arrest beginning at 1 uM, which increased as the dose was escalated. Similar results were seen using the CDK inhibitor, flavopiridol (not shown). VMY treatment also increased the subG_1 population of cells, consistent with DNA fragmentation and apoptotic cell death following treated with VMY. Treatment of DAOY cells with either LY294002 or PVB failed to significantly alter the sub-G_1 population of cells (**Fig. 1A**). Similar results were seen in D556 cells, with VMY inducing a significant G_2/M arrest beginning at 0.5 uM and an increased subG_1 fraction beginning at 5.0 uM (**Fig. 1B**). Both VMY and the CDK inhibitor flavopiridol, but neither PVB nor the dansyl group alone, significantly induced cell death in DAOY cells at 18 h as measured by trypan blue dye exclusion (**Fig. 2A**). Furthermore, VMY had no effect on cell cycle progression or apoptosis in NIH3T3 cells (**Fig. S1A**), similar to our previous results in non-transformed prostate and breast cancer cell lines.[13,14] The ED_{50}'s (effective doses necessary to achieve 50% cell death) for VMY and flavopiridol were approximately 76 and 30.5 uM, respectively (**Fig. S1B and C**)

VMY induces apoptosis via increased levels of pro-apoptotic proteins and caspase activity. Using antibody proteome arrays we previously reported that VMY induced apoptosis in LNCaP prostate cancer cells in part through an induction of p53 and the intrinsic apoptotic pathway.[13] To investigate the mechanisms by which VMY regulated apoptosis in DAOY cells, similar experiments were performed. VMY significantly increased the protein levels of the death receptors DR4 and DR5, which are required for TRAIL-dependent induction of apoptosis in cancer cells. Levels of the Fas ligand TNFSF6 and cleaved caspase-3 (c-casp-3), the active form generated by proteolytic maturation, were also increased (**Fig. 2B**). The phosphorylation status of p53 serine residues 15, 46 and 392, which were induced by VMY in LNCaP cells,[13] were unaffected in DAOY cells (not shown). Levels of the proapoptotic proteins BAD and BAX were induced while levels of the antiapoptotic regulatory protein cIAP/Birc2 were modestly reduced (**Fig. 2B**).

Protein gel blots were run to assess the effect of VMY on levels of the CDK inhibitory protein $p21^{CIP1/WAF1}$, of cyclins E and B1 as well as PARP status (**Fig. 2C**). VMY, but not PVB, significantly increased the levels of cleaved PARP while levels of the G_1/S protein, cyclin E, were not changed. Surprisingly, while $p21^{CIP1}$ levels which were induced by VMY in LNCaP cells[13] and by low concentrations of VMY in DAOY cells (**Fig. 2C**), decreased by 82% (±3, n = 3) and 90% (±7, n = 3) with 10 and 30 μm VMY, respectively (**Fig. 2C**). Treatment with flavopiridol also significantly decreased $p21^{CIP1/WAF1}$ (**Fig. S1D**). The levels of cyclin B were marginally reduced by VMY at 10 and 30 uM (**Fig. 2C**).

VMY inhibits CDK1 activity in DAOY cells. Our recent data using purified cyclin/CDK complexes established that VMY was a potent inhibitor of the cyclinB/CDK1 complex.[14]

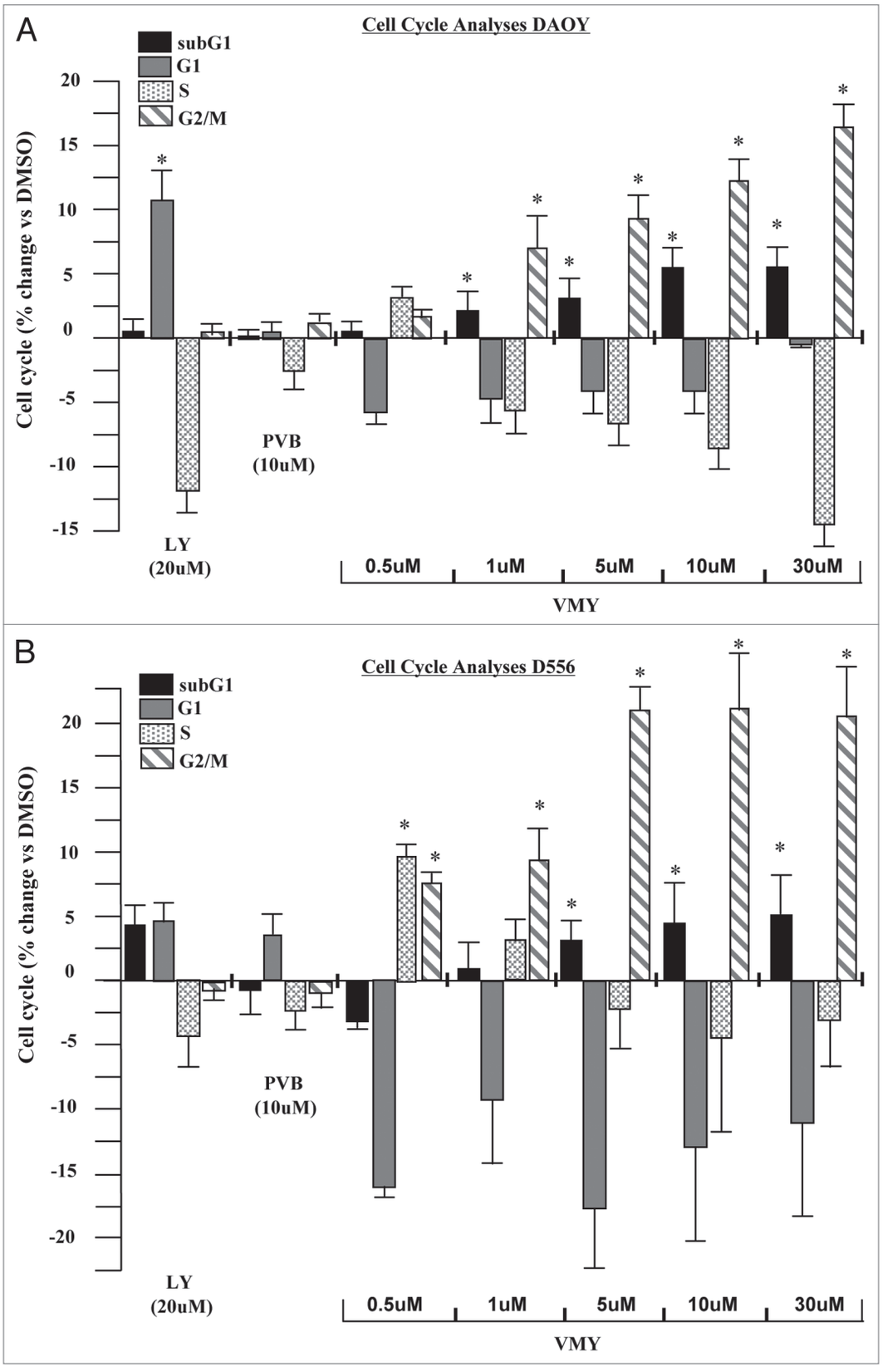

Figure 1. Effects of VMY on cell cycle progression in human medulloblastoma cells. The human medulloblastoma cell lines (A), DAOY or (B) D556 were treated for 18 h with either LY294002 (LY), purvalanol B (PVB) or VMY at the concentrations shown. Cells were harvested and both DNA fragmentation (subG$_1$) and the cell cycle profile were measured by flow cytometry. Data are average ± standard deviation of n ≥ three separate experiments vs. DMSO.

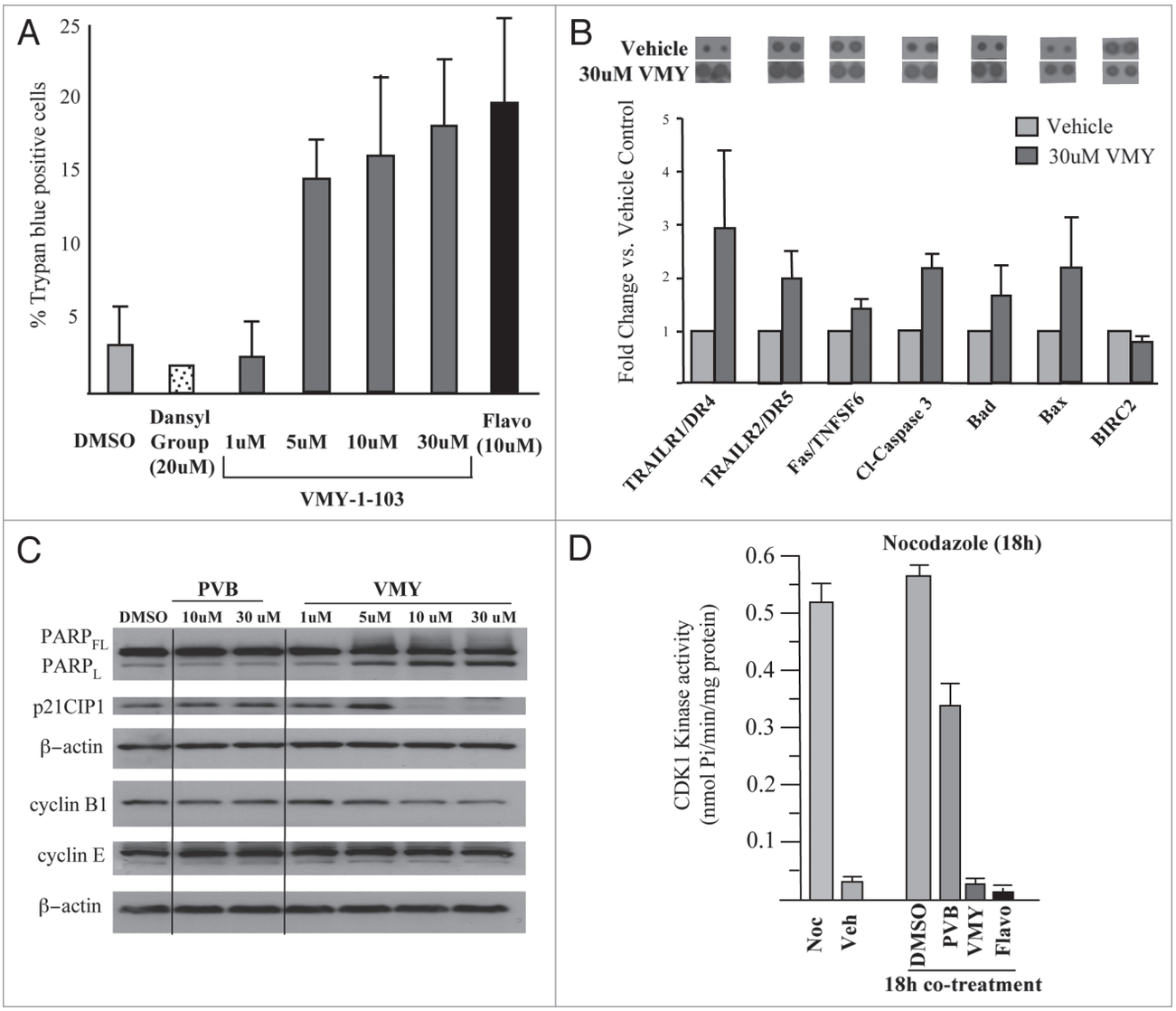

Figure 2. Effects of VMY on DAOY cell proliferation. (A) DAOY cells were treated for 18 h with either DMSO, the dansyl group alone or VMY-1-103 at the concentrations shown. Cells were harvested and cell viability assessed by trypan blue dye exclusion on >300 cells. Data are average ± standard deviation of n ≥ three separate experiments. (B) Apoptosis proteome arrays performed on extracts from DAOY cells were treated for 18 h with either DMSO or VMY at 30 uM. Fold change in protein abundance vs. DMSO are shown as Ave ± deviation of duplicate samples from n = two separate experiments. A representative proteomic array is shown at top. (C) Representative protein gel blot (n ≥ 3) performed on DAOY cells treated for 18 h with either PVB or VMY at the concentrations shown. (D) In vitro CDK1-kinase assays performed on DAOY cell extracts treated as marked. Data are percent inhibition in substrate phosphorylation vs. vehicle control for n = two experiments. Flavo, Flavopiridol; Cl^- capase-3, cleaved caspase-3; $PARP_{FL}$, full length PARP; $PARP_L$, 89 kD fragment of cleaved PARP; Noc, nocodazole; Veh, vehicle.

We therefore assessed the CDK-inhibitory capacity of VMY in protein extracts from treated DAOY cells. The catalytic activity of CDK1 in the cell extract was assessed using an in vitro kinase reaction with the CDK1 peptide target substrate (ADA QHA TPP KKK RKV ED). Intracellular CDK1 activity was initially quantified using extracts from randomly cycling cells or in cells synchronized in the G_2-phase of the cell cycle with nocodazole. The CDK1-kinase activity in randomly cycling cells was less than 0.1 nmol of phosphate utilized per minute (0.035 nmol/min/mg ± 0.005, n = 3), which increased 15-fold in cells synchronized with nocodazole (to 0.522 nmol/min/mg ± 0.3, n = 4) (**Fig. 2D**). CDK1-kinase assays were next performed on extracts from DAOY cells co-treated for 18 h with nocodazole and either DMSO, PVB (30 um), VMY (30 um) or flavopiridol (10 uM). Both VMY and flavopiridol inhibited CDK1 activity by over 90% (**Fig. 2D**), vs. a 33% inhibition by PVB.

VMY delays progression through mitosis. Orderly regulation of the cyclinB/CDK1 complex is required for entry into mitosis.[15] As VMY was able to significantly inhibit CDK1 activity in DAOY cells, we next assessed whether a component of VMY's antiproliferative activity was associated with an inhibition of mitotic progression. To help determine how VMY blocked cell division, DAOY cells were stably transfected with histone-H2B-GFP (DAOY/H2B-GFP, described in the Methods section) to enable

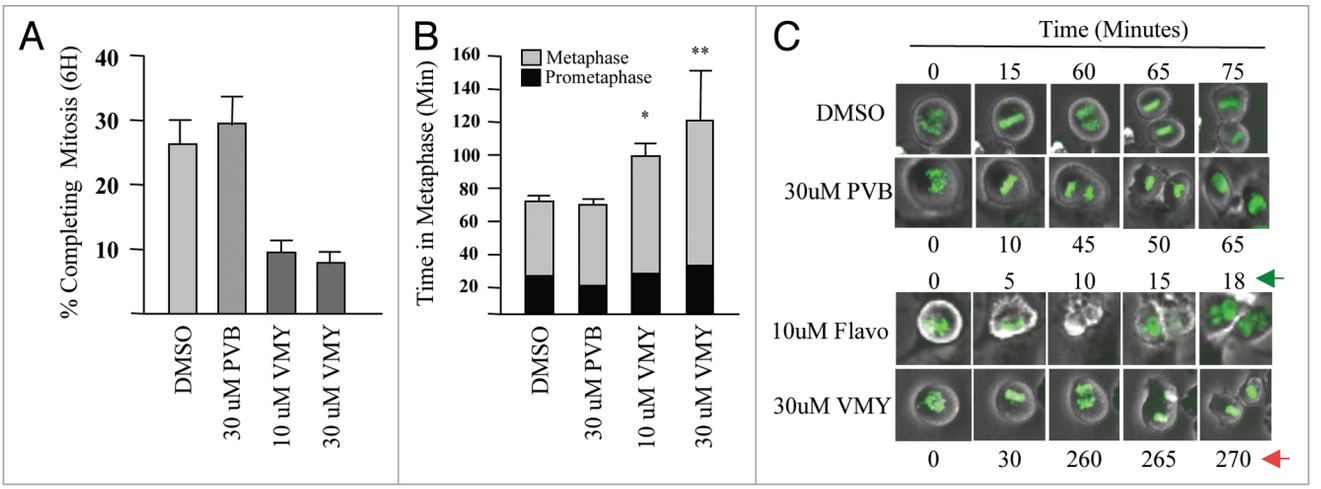

Figure 3. VMY-induced disruption of mitosis in DAOY cells. Live cell imaging was performed using stably transfected DAOY/GFP-H2B cells. (A) The percent of cells that successfully completed mitosis within 6 h following release from nocodazole block. (B) Metaphase transit time. (C) Examples of transit times of cells that successfully progressed through metaphase. Data are average percent change (+ SD, n > 250 cells, two separate experiments). Arrows, significant changes in mitotic progression in VMY vs. Flavo (flavopiridol) treated cells.

visualization of chromosomal activity in living cells using time lapsed video microscopy. DAOY/H2B-GFP cells were synchronized with nocodazole for 18 h, resulting in more than 90% of the cells arresting in G_2 (not shown). Nocodazole was removed from the cells followed by fresh culture media containing either DMSO, PVB, flavopiridol or VMY. The time of progression through mitosis was quantified by live cell imaging using a Nikon Eclipse TE300 video microscope. By 6 h, 26% of control, and 28% of the PVB-treated DAOY/H2B-GFP cells underwent an orderly progression from prophase through metaphase into telophase (**Fig. 3A and C**). Treatment with flavopiridol resulted in a significant acceleration of mitotic progression (**Fig. 3C**). This acceleration, or "mitotic slippage," is frequently seen with CDK inhibitors such as purvalanol, roscovitine or flavopiridol,[16] and is the result the inhibition of cyclinB/CDK1 activity during mitosis.[17] Conversely, treatment with VMY significantly reduced the number of cells completing mitosis within 6 h to less than 10% at 30 uM (**Fig. 3A**), and significantly prolonged metaphase vs. PVB or vehicle (**Fig. 3B and C**). Stage-specific analyses of the mitotic transit times established that while treatment with 30 uM PVB resulted in a slight acceleration in the prophase to metaphase progression (**Fig. 4A**), treatment with VMY significantly delayed both the prophase to metaphase and metaphase to anaphase transitions (**Fig. 4A and B**). Similar results were seen in D556 cells, where VMY significantly delayed mitotic progression (**Fig. 5A and B**) while flavopiridol significantly shortened time in mitosis (**Fig. 5A and B**), which is again consistent with its ability to induce mitotic slippage.

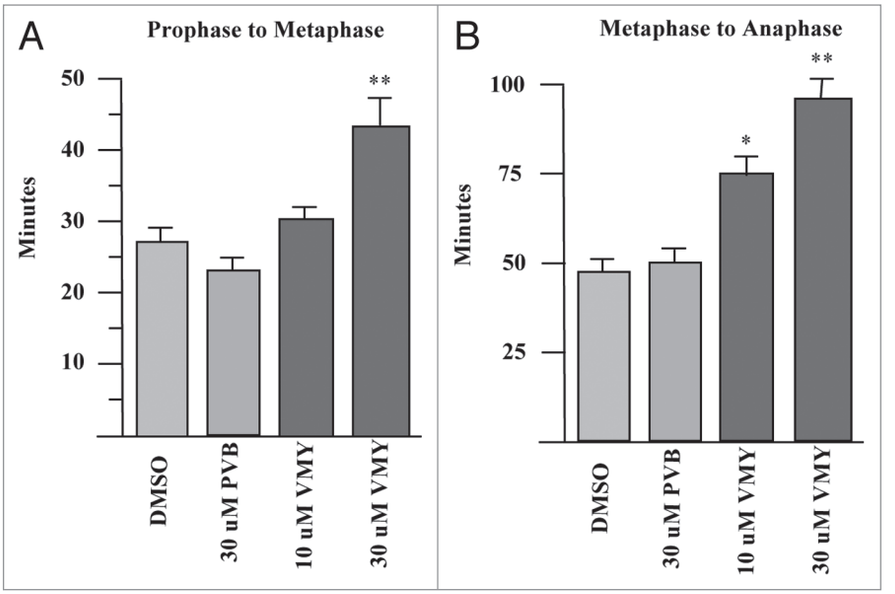

Figure 4. VMY delays progression through mitosis. DAOY/GFP-H2B cells were released from nocodazole block and followed by live-cell video microscopy. Time of progression from (A) prophase to metaphase and (B) metaphase to anaphase. *p ≤ 0.05, **p ≤ 0.01.

VMY treatment disrupts centrosome polarity and induces mislocalization of chromosomes. The Aurora-family of kinases is comprised of three genes *(aurka, aurkb* and *aurkc*) and Aurora Kinase A localizes to the centrosomes and spindle poles and regulates spindle assembly and centrosome maturation.[18] Aurora Kinase B acts in part to correct for misaligned chromosomes during mitosis,[19] and histone H3 that has been phosphorylated on serine 10 (p-HH3) by Aurora Kinase B is a marker of mitotic activity. The Wee1 kinase is a spindle pole associated protein during the G_2/M transition. Wee1 functions to regulate progression from G_2 into mitosis by inhibiting the activity of the cyclin

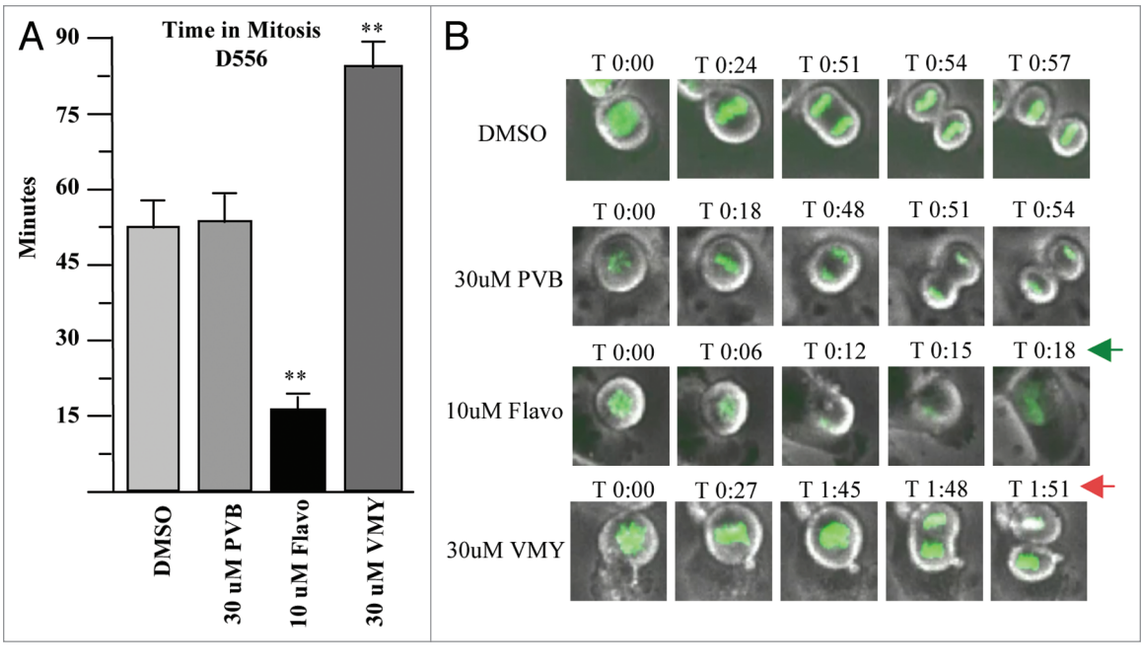

Figure 5. Effects of VMY and flavopiridol on Mitosis in D556 cells. Stable GFP-H2B/D556 cells were treated with nocodazole for 18 h. The nocodazole was removed and the cells were treated with the compounds as shown and followed by live cell imaging. (A) Average, n = four experiments. (B) Representative live cell images. **p < 0.01. Arrows, significant changes in mitotic progression in VMY vs. Flavo (flavopiridol) treated cells.

B/CDK1 holoenzyme complex via phosphorylation of CDK1 on tyrosines 14 and 15.

Based on our observations that VMY delayed the progression through mitosis, and to begin to understand the effect that VMY was having on the mitotic apparatus, randomly-cycling control and inhibitor-treated DAOY cells where probed with anti-Aurora A and p-HH3 antibodies and were counterstained with both phalloidin for F-actin and DAPI for chromatin.

In control cells, Aurora Kinase A immunofluorescence was centrally located within the chromatin during prometaphase, and was associated with the polar centrosome structures as the cells progressed into metaphase (**Fig. 6A**, *PM* and *M* respectively), consistent with its normal mitotic localization. The signal for p-HH3 localized to the end of the condensed chromosomes as expected (**Fig. 6A**). In contrast, within 1 h of treatment with VMY, mitotic abnormalities were evident, with cells exhibiting a disorganized alignment of the chromosomes (**Fig. 6B**, *PM* and *A*). In addition, while Aurora Kinase A staining remained localized to the centrosome, treatment with VMY resulted in a mislocalization of p-HH3 during all stages of mitosis (**Fig. 6B**). In those cells that were able to progress through metaphase, abnormalities such as lagging chromosomes persisted (**Fig. 6B**, *A* and *T*).

Control cells stained with Aurora Kinase A and phosphoserine 53-WEE1 andibodies, DAPI and phalloidin exhibited colocalized Aurora kinase A and Wee1 within the centrosome (**Fig. 6C**). While centrosome polarity was disrupted during prometaphase and metaphase, treatment with VMY did not appear to disrupt Aurora kinase A and Wee1 colocalization, despite its effect on chromosomal organization and migration. Protein gel blotting performed on extracts from DAOY cells treated for 1 h with PVB, VMY or flavopiridol following release from an 18 h nocodazole block established that the abundance tyrosine-15-phosphorylated CDK1 was not significantly affected by treatment with PVB, VMY or flavopiridol (**Fig. S2**), suggesting that VMY was not inhibiting Wee1 kinase activity during that time period. Aurora Kinase A levels were not affected by VMY or PVB, but were decreased following 1 h treatment with flavopiridol (**Fig. S3**), perhaps due to the mitotic slippage induced by flavopiridol.

Discussion

Like many cancers, the etiology of MB is diverse, and a complex array of developmental and cell cycle regulatory genes, proteins and signaling pathways have been found to be compromised in both clinical samples[4-6] and in animal models.[20,21] Regardless of the underlying genetic or molecular abnormality, these tumors are highly proliferative, and advances in clinical treatment will require developing therapies that effectively target critical components of the cell proliferation machinery. This approach is underscored by the observation that Hh signaling pathway inhibitors such as GDC-0449, while initially successful in treating adult MB, induced or supported activating somatic mutations that ultimately resulted in disease recurrence.[22] We[9] and others[23] have recently explored the possibility that inhibiting the transcription factor, Gli, with arsenic trioxide may effectively block MB proliferation in culture and in mouse models of MB.

In the present report, we describe the effects of a new CDK-inhibitor developed by our group on cell proliferation and apoptosis in human medulloblastoma cell lines. Collectively the data

presented indicate that VMY induced cell cycle arrest and induced apoptosis at concentrations that were significantly lower than its parent compound, PVB, consistent with our previous studies.[13,14] VMY was also capable of significantly inhibiting CDK1 kinase activity but while flavopiridol induced mitotic slippage, VMY significantly delayed completion of prometaphase and metaphase, in part through interfering with chromosomal organization, thereby disrupting the orderly progression through mitosis. We conclude that a component of VMY's antiproliferative activity is the result of an induction of induction of apoptosis during mitosis, a process that has been referred to as mitotic catastrophe.[24]

The cyclin B/CDK1 complex is a key regulator of cell division. Orderly progression from G_2 to M requires a phosphorylation-dependent inhibition of CDK1 on Thr14 and Tyr 15 by Wee1/MYT1 in G_2, enabling the proper timing of entry into mitosis. As cells progress into M, the cyclin B/CDK1 complex is activated via dephosphorylation of the CDK1 Thr14 and Tyr 15 residues by the Cdc25C phosphatase. For cells to continue to progress through metaphase and complete cell division, cyclin B/CDK1 activity has to again be suppressed, occurring through degradation of cyclin B via the APC/C complex and the ubiquitin/proteosome pathway.[25] Because the suppression of cyclin B/CDK1 activity during mitosis is prerequisite for M-phase progression, CDK1 inhibitors such as PVB and flavopiridol have been found to induce mitotic slippage and accelerate mitosis and cytokinesis. For example, experiments performed in mitotically inhibited HeLa cells established that inhibition of CDK1 with PVB resulted in an accelerated mitotic exit and premature cytokinesis.[26] Mitotic slippage was also seen in taxane-inhibited cells treated with flavopiridol.[27] It is generally believed that mitotic slippage inhibits M-phase apoptosis but can result in G_1 arrest and apoptosis due to anueploidy.[28] We found that while treatment of MB cells with flavopiridol, and to a much lesser extent purvalanol B, resulted mitotic slippage, VMY not only failed to affect mitotic slippage, but induced a prolonged prometaphase/metaphase arrest which was due, at least in part, to a loss of normal chromosomal localization.

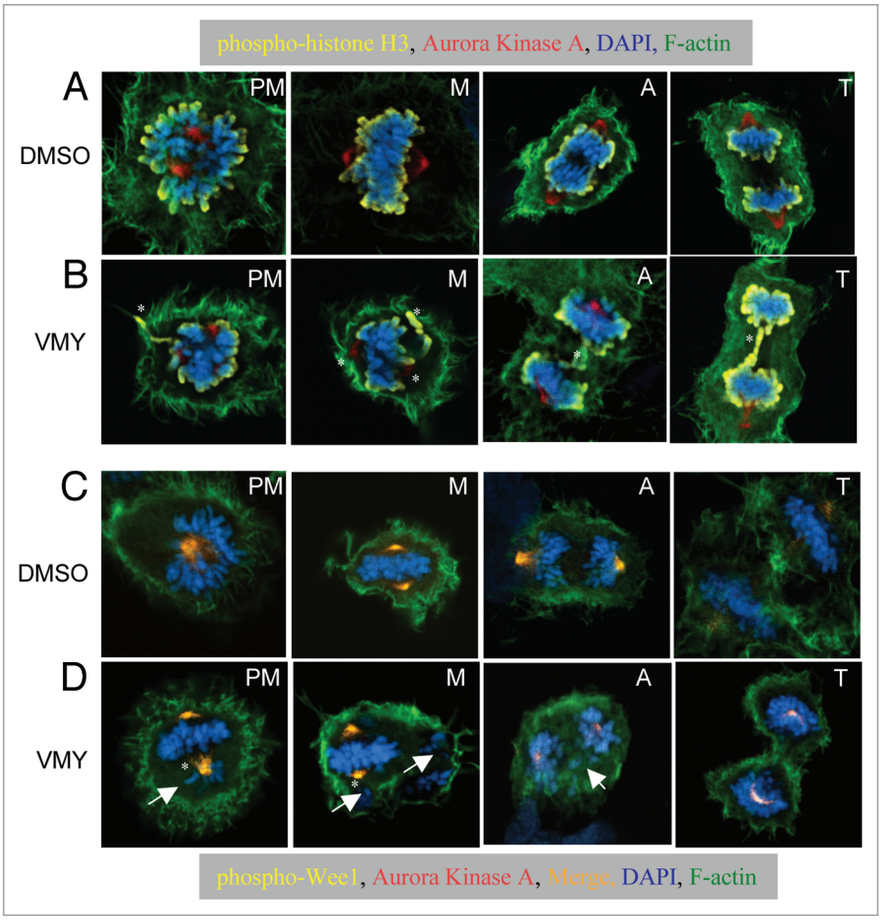

Figure 6. Merged fluorescent imaging of DAOY cells. Cells were treated DMSO or VMY (30 um) for 1 h. (A and B) Cells were stained with phospho-histone H3 (yellow) and Aurora Kinase A antibodies (red) as well as with DAPI (blue) and phalloidin for F-actin (green). (C and D) Cells were stained with phospho-Wee1 (yellow) and Aurora Kinase A antibodies (red) as well as with DAPI (blue) and phalloidin for F-actin (green). The Wee1/Aurora A merge is in orange. PM, prometaphase; M, metaphase; A, anaphase; T, telophase. Arrows, trailing or misaligned chromosomes, *, mislocalized Wee1, Aurora Kinase A or phospho-histone H3.

VMY, like roscovitine and flavopiridol, can inhibit the CDK7/CAK and CDK9/Cyclin T1 kinases in vitro[14] which affect transcription via a phosphorylation-dependent regulation of the c-terminal domain of RNA polymerase II. The *cyclin D1* and *p21$^{CIP1/WAF1}$* genes are known targets. We have shown that protein abundance of p21$^{CIP1/WAF1}$ was significantly decreased by VMY (**Fig. 2**) and as well as by flavopiridol (**Fig. S1**). Cyclin D1 levels also were reduced (Ringer L, Albanese C, unpublished) however no change in the G_1 fraction of cells was observed (**Fig. 1**). The functional consequences of the reduction of these proteins and whether regulation occurs at the level of RNA polymerase II is not known at this time. Hyperphosphorylated p21$^{CIP1/WAF1}$ has been shown to activate the CDK1/Cyclin B complex during the G_2/M transition[29] and a loss of p21$^{CIP1/WAF1}$ may delay mitosis. However, since both VMY and flavopiridol cause a similar reduction in protein levels, the loss of p21$^{CIP1/WAF1}$ cannot explain the differential effects on mitotoic progression seen between the two compounds.

While VMY does not appear to promote a complete disorganization of the centrosome, alterations were clearly evident, including compromised polarity. Defects in centrosome structure or function can have profound influences on mitosis, and cells that undergo a prolonged mitotic arrest become susceptible to mitotic apoptosis, which occurs when a cell is unable to fulfill its spindle checkpoint function. Commonly used chemotherapeutic agents such as the taxanes and vincristine, as well as inhibitors of key

mitosis-related kinases, such as the Aurora or Polo-like kinases, induce mitotic apoptosis through disruption of the mitotic spindle (reviewed in ref. 30), highlighting the mitotic checkpoint as a target for intervention. While the mechanisms by which VMY interfered with both chromosome alignment during metaphase and their migration during anaphase and telophase are not yet known, the rapid mitotic disruption observed with VMY clearly differentiates this compound from its parent, PVB, as well as from flavopiridol. These non-classical spindle-disrupting capabilities of VMY in combination with its classical CDK-inhibitory activity suggest that VMY represents a new sub-class of small molecule CDK inhibitor. Our data warrant further investigations into the anti-mitotic mechanisms of action of VMY both in vitro and in preclinical MB models.[9]

Materials and Methods

Cell lines and cell culture. The human medulloblastoma cell lines, DAOY and D556 were maintained in RPMI, with 10% FCS, 0.1 mM non-essential amino acids, 100 U/ml Penicillin-Streptomycin and 1 mM sodium pyruvate at 37°C in 5% CO_2 as previously described in references 9 and 10. The PI3K inhibitor LY294002 (Sigma), the parent CDK inhibitor purvalanol B (Sigma), flavopiridol (Sigma), or VMY-1-103,[13,14] were added to the culture medium for up to 18 h. DMSO was used as vehicle control. The ED_{50}s were calculated using Prism (GraphPad). To label chromatin, DAOY cells were stably transfected with pEGFP-N1-Histone2B-GFP plasmid (a gift from Susette Mueller). Briefly, a 10 cm dish of DAOY cells was transfected with 10 μg of GFP/H2B in media containing 10% FBS using fugene 6 (Roche). After 48 h, the cells were split into three 10 cm dishes and 400 μg/ml G418 (Invitrogen) was added. Positive colonies were identified by fluorescence microscopy and six individual clones were selected. The cells were treated with VMY followed by cell cycle analyses and comparisons were made to untransfected cells to ensure there were no changes in the cells sensitivity to the drug.

Flow-cytometry. The medulloblastoma cells were collected by trypsinization, fixed in 10% ethanol and resuspended in PBS containing 20 μg/ml propidium iodide (PI) and 5 U RNase A. DNA content was measured using a FACStar Plus dual laser FACSort system (Becton-Dickinson) as previously described in references 13, 31 and 32.

Immunoblotting. Protein extracts were separated on 4–20% Tris-glycine gels and electro-blotted onto nitrocellulose.[13,33] Protein levels were assessed using antibodies against cyclin B1, cleaved caspase-3 and PARP and $p21^{CIP1}$, as previously described in reference 13. Anti-β-actin (Cell Signaling, 4967) was used as loading control as previously described in reference 13.

Cell viability and growth. Following inhibitor treatment, cell viability was determined by trypan blue exclusion. For apoptosis assays, Proteome Profiler human apoptosis arrays (R&D Systems) were performed as previously described in reference 13 as per the manufacturer's protocol. Briefly, nitrocellulose membranes (spotted with 35 antibodies, in duplicate) were blocked with array buffer (supplied by the manufacturer) for 1 h at room temperature, the membranes were washed and incubated with 500 μg of protein overnight at 4°C. A biotinylated primary antibody (supplied by the manufacturer) was added for 1 h, followed by a 30 min incubation with Streptavidin-HRP, and finally with an ECL reagent (1:3,000; Pierce). Array data were developed on X-ray film and spot areas and intensities were analyzed using ImageJ (NIH) as previously described in reference 13.

Fluorescence imaging. Cells were seeded on glass coverslips and treated with DMSO or inhibitors for 1 h. Cells were washed with PBS and fixed in 10% formalin for 10 min. Cells were then washed three times with PBS, permeabilized with 0.1% Triton X-100, and washed an additional three times with PBS. Cells were then incubated with the following primary antibodies: p-Wee1 (Ser 53, 1:50, Santa Cruz), Aurora A (1:100, BD Biosciences), and p-Histone H3 (S10, 1:200, Cell Signaling) for 1 hr at room temperature. Slides were then washed with PBS an additional three times and stained with the following secondary antibodies for 30 min at room temperature: Cy5 donkey anti-rabbit (1:200, Invitrogen) and Texas Red donkey anti-mouse (1:200). Slides were then counterstained with DAPI and 488-Phalloidin (1:200, Invitrogen) for 5 min. The coverslips were mounted onto glass slides with Tris-buffered fluoro-gel (Electron Microscopy Sciences). Confocal microscopy was performed on an Olympus Fluoview-FV300 Laser Scanning Confocal System (100x lens, oil immersion).

Live cell imaging. Automated time-lapse microscopy was performed on a Nikon Eclipse TE-300 Inverted Spinning Disc Confocal Microscope System. Cells were maintained in a microscope stage incubator at 37°C in a humidified atmosphere of 5% CO_2 throughout the experiment. Confocal microscopy was performed using a 40x lens. Images and time-lapse videos were obtained using Velocity (v 5.3.1) image acquisition and analysis software by Improvision. To image time in mitosis, stable GFP-H2B DAOY cells were seeded in a 12-well glass-bottom dish (MatTek) and were synchronized in the G_2 phase of the cell cycle with 20 ng/ml nocodazole for 12 h. Ten to twenty cells were selected in each well using the Velocity software, and imaged in the presence of nocodazole. Media containing nocodazole was then removed from the dish and the cells were washed three times with PBS. Cell culture media was replaced containing DMSO, Purvalanol B, Flavopiridol or VMY-1-103. Cells were immediately imaged every 2 min for 12 h. Ten Z-stack sections were taken images were taken per cell (3 uM spacing between slices) with a GFP (488 nm) laser. One bright-field image was taken in the center of each cell as a reference point. Mitotic cells were quantified and manually analyzed for time in mitosis.

Cdk1 kinase assays. Ten centimeter dishes of 80% confluent DAOY cells were placed on ice for 10 min and scraped into the culture medium. The cells were collected by centrifugation for 5 min at 500 g, washed with 10 ml PBS containing 1 mM $MgCl_2$ and resuspended in 1.0 ml kinase assay buffer (25 mM β-glycerophosphate, 25 mM (4-(2-hydroxyethyl)-1-piperazineethanesulfonic acid)-KOH (pH 7.4), 10 mM $MgCl_2$, 5 mM ethylene glycol tetraacetic acid, 1 mM dithiothreitol,

0.5 mM phenylmethylsulfonyl fluoride, 0.1 mM Na_3VO_4, 1 μg/ml aprotinin, 1 μg/ml leupeptin, 1 μg/ml pepstatin) at 4°C. Lysates were prepared using ultrasonic disruption at 4°C and immediately assayed for kinase activity. For each lysate, parallel assays were performed for 12 min at 33°C in the presence and absence of 0.1 mM CSH103 cdk1 substrate peptide (ADA QHA TPP KKK RKV ED; Enzo Life Sciences), and included (in a total volume of 100 μl) 10–20 μl lysate, 0.1 mM ATP and 0.1 mCi/ml γ-[^{32}P]ATP (7,000 Ci/mmol; MP Biomedicals). To determine levels of phosphorylation, 25 μl aliquots of assays were spotted on 2.3 cm P81 cellulose phosphate filters (Whatman) followed by five washes with 100 ml 1% (v/v) H_3PO_4 (≥5 min per wash). Washed filters were transferred to 20 ml glass vials for scintillation counting following addition of 10 ml BioSafe II scintillation cocktail (Research Products International). Counts were normalized for [^{32}P]ATP specific activity and lysate protein concentration; determined using the Bio-Rad protein assay with a bovine IgG standard.

Disclosure of Potential Conflicts of Interest

A patent application has been filed by Georgetown University on the behalf of the inventors Venkata Yenugonda and Milton L. Brown that are listed as authors in this article.

Acknowledgments

We thank the Flow Cytometry and the Microscopy and Imaging Shared Resources of the Georgetown Lombardi Comprehensive Cancer Center. We thank Susette Mueller for the EGFP Histone H2B expression vector and for her help and expertise related to live cell imaging. This work was supported by the Georgetown Drug Discovery Program and by P30 CA51008, R01CA129003 (C.A.), ABC2 (C.A. and T.M.).

Note

Supplemental materials can be found at:
www.landesbioscience.com/journals/cbt/article/17682/.

References

1. Hatten ME, Roussel MF. Development and cancer of the cerebellum. Trends Neurosci 2011; 34:134-42; PMID:21315459; DOI:10.1016/j.tins.2011.01.002.
2. Saury JM, Emanuelson I. Cognitive consequences of the treatment of medulloblastoma among children. Pediatr Neurol 2011; 44:21-30; PMID:21147383; DOI:10.1016/j.pediatrneurol.2010.07.004.
3. Roussel MF, Robinson G. Medulloblastoma: advances and challenges. F1000 Biol Rep 2011; 3:5; PMID:21655335; DOI:10.3410/B3-5.
4. Kool M, Koster J, Bunt J, Hasselt NE, Lakeman A, van Sluis P, et al. Integrated genomics identifies five medulloblastoma subtypes with distinct genetic profiles, pathway signatures and clinicopathological features. PLoS ONE 2008; 3:3088; PMID:18769486; DOI:10.1371/journal.pone.0003088.
5. Northcott PA, Korshunov A, Witt H, Hielscher T, Eberhart CG, Mack S, et al. Medulloblastoma Comprises Four Distinct Molecular Variants. J Clin Oncol 2011; 29:1408-14; PMID:20823417; DOI:10.1200/JCO.2009.27.4324.
6. Cho YJ, Tsherniak A, Tamayo P, Santagata S, Ligon A, Greulich H, et al. Integrative genomic analysis of medulloblastoma identifies a molecular subgroup that drives poor clinical outcome. J Clin Oncol 2011; 29:1424-30; PMID:21098324; DOI:10.1200/JCO.2010.28.5148.
7. Marino S. Medulloblastoma: developmental mechanisms out of control. Trends Mol Med 2005; 11:17-22; PMID:15649818; DOI:10.1016/j.molmed.2004.11.008.
8. Bar EE, Chaudhry A, Farah MH, Eberhart CG. Hedgehog signaling promotes medulloblastoma survival via Bc/II. Am J Pathol 2007; 170:347-55; PMID:17200206; DOI:10.2353/ajpath.2007.060066.
9. Beauchamp EM, Ringer L, Bulut G, Sajwan KP, Hall MD, Lee YC, et al. Arsenic trioxide inhibits human cancer cell growth and tumor development in mice by blocking Hedgehog/GLI pathway. J Clin Invest 2011; 121:148-60; PMID:21183792; DOI:10.1172/JCI42874.
10. Abouantoun TJ, Castellino RC, MacDonald TJ. Sunitinib induces PTEN expression and inhibits PDGFR signaling and migration of medulloblastoma cells. J Neurooncol 2011; 101:215-26; PMID:20524040; DOI:10.1007/s11060-010-0259-9.
11. Pestell RG, Albanese C, Reutens AT, Segall JE, Lee RJ, Arnold A. The cyclins and cyclin-dependent kinase inhibitors in hormonal regulation of proliferation and differentiation. Endocr Rev 1999; 20:501-34; PMID:10453356; DOI:10.1210/er.20.4.501.
12. Chang YT, Gray NS, Rosania GR, Sutherlin DP, Kwon S, Norman TC, et al. Synthesis and application of functionally diverse 2,6,9-trisubstituted purine libraries as CDK inhibitors. Chem Biol 1999; 6:361-75; PMID:10375538; DOI:10.1016/S1074-5521(99)80048-9.
13. Ringer L, Yenugonda VM, Ghosh A, Divito K, Trabosh V, Patel Y, et al. VMY-1-103, a dansylated analog of purvalanol B, induces caspase-3-dependent apoptosis in LNCaP prostate cancer cells. Cancer Biol Ther 2010; 10:320-5; PMID:20574155; DOI:10.4161/cbt.10.4.12208.
14. Yenugonda VM, Deb TB, Grindrod SC, Dakshanamurthy S, Yang Y, Paige M, et al. Fluorescent cyclin-dependent kinase inhibitors block the proliferation of human breast cancer cells. Bioorg Med Chem 2011; 19:2714-25; PMID:21440449; DOI:10.1016/j.bmc.2011.02.052.
15. Lindqvist A, Rodriguez-Bravo V, Medema RH. The decision to enter mitosis: feedback and redundancy in the mitotic entry network. J Cell Biol 2009; 185:193-202; PMID:19364923; DOI:10.1083/jcb.200812045.
16. Potapova TA, Sivakumar S, Flynn JN, Li R, Gorbsky GJ. Mitotic progression becomes irreversible in prometaphase and collapses when Wee1 and Cdc25 are inhibited. Mol Biol Cell 2011; 22:1191-206; PMID:21325631; DOI:10.1091/mbc.E10-07-0599.
17. Shapiro GI. Cyclin-dependent kinase pathways as targets for cancer treatment. J Clin Oncol 2006; 24:1770-83; PMID:16603719; DOI:10.1200/JCO.2005.03.7689.
18. Lens SM, Voest EE, Medema RH. Shared and separate functions of polo-like kinases and aurora kinases in cancer. Nat Rev Cancer 2010; 10:825-41; PMID:21102634; DOI:10.1038/nrc2964.
19. Lampson MA, Cheeseman IM. Sensing centromere tension: Aurora B and the regulation of kinetochore function. Trends Cell Biol 2011; 21:133-40; PMID:21106376; DOI:10.1016/j.tcb.2010.10.007.
20. Saab R, Rodriguez-Galindo C, Matmati K, Rehg JE, Baumer SH, Khoury JD, et al. $p18^{Ink4c}$ and p53 Act as tumor suppressors in cyclin D1-driven primitive neuroectodermal tumor. Cancer Res 2009; 69:440-8; PMID:19147556; DOI:10.1158/0008-5472.CAN-08-1892.
21. Ayrault O, Zindy F, Rehg J, Sherr CJ, Roussel MF. Two tumor suppressors, $p27^{Kip1}$ and patched-1, collaborate to prevent medulloblastoma. Mol Cancer Res 2009; 7:33-40; PMID:19147535; DOI:10.1158/1541-7786.MCR-08-0369.
22. Yauch RL, Dijkgraaf GJ, Alicke B, Januario T, Ahn CP, Holcomb T, et al. Smoothened mutation confers resistance to a Hedgehog pathway inhibitor in medulloblastoma. Science 2009; 326:572-4; PMID:19726788; DOI:10.1126/science.1179386.
23. Kim J, Lee JJ, Kim J, Gardner D, Beachy PA. Arsenic antagonizes the Hedgehog pathway by preventing ciliary accumulation and reducing stability of the Gli2 transcriptional effector. Proc Natl Acad Sci USA 2010; 107:13432-7; PMID:20624968; DOI:10.1073/pnas.1006822107.
24. Galluzzi L, Aaronson SA, Abrams J, Alnemri ES, Andrews DW, Baehrecke EH, et al. Guidelines for the use and interpretation of assays for monitoring cell death in higher eukaryotes. Cell Death Differ 2009; 16:1093-107; PMID:19373242; DOI:10.1038/cdd.2009.44.
25. Ma HT, Poon RY. How protein kinases co-ordinate mitosis in animal cells. Biochem J 2011; 435:17-31; PMID:21406064; DOI:10.1042/BJ20100284.
26. Niiya F, Xie X, Lee KS, Inoue H, Miki T. Inhibition of cyclin-dependent kinase 1 induces cytokinesis without chromosome segregation in an ECT2 and MgcRacGAP-dependent manner. J Biol Chem 2005; 280:36502-9; PMID:16118207; DOI:10.1074/jbc.M508007200.
27. Shapiro EM, Skrtic S, Sharer K, Hill JM, Dunbar CE, Koretsky AP. MRI detection of single particles for cellular imaging. Proc Natl Acad Sci USA 2004; 101:10901-6; PMID:15256592; DOI:10.1073/pnas.0403918101.
28. Blagosklonny MV. Mitotic arrest and cell fate: why and how mitotic inhibition of transcription drives mutually exclusive events. Cell Cycle 2007; 6:70-4; PMID:17245109; DOI:10.4161/cc.6.1.3682.
29. Dash BC, El-Deiry WS. Phosphorylation of p21 in G_2/M promotes cyclin B-Cdc2 kinase activity. Mol Cell Biol 2005; 25:3364-87; PMID:15798220; DOI:10.1128/MCB.25.8.3364-87.2005.
30. Vakifahmetoglu H, Olsson M, Zhivotovsky B. Death through a tragedy: mitotic catastrophe. Cell Death Differ 2008; 15:1153-62; PMID:18404154; DOI:10.1038/cdd.2008.47.
31. Albanese C, D'Amico M, Reutens AT, Fu M, Watanabe G, Lee RJ, et al. Activation of the *cyclin D1* gene by the E1A-associated protein p300 through AP-1 inhibits cellular apoptosis. J Biol Chem 1999; 274:34186-95; PMID:10567390; DOI:10.1074/jbc.274.48.34186.
32. Albanese C, Wu K, D'Amico M, Jarrett C, Joyce D, Hughes J, et al. IKKalpha Regulates Mitogenic Signaling through Transcriptional Induction of Cyclin D1 via Tcf. Mol Biol Cell 2003; 14:585-99; PMID:12589056; DOI:10.1091/mbc.02-06-0101.
33. Casimiro M, Rodriguez O, Pootrakul L, Aventian M, Lushina N, Cromelin C, et al. ErbB-2 induces the cyclin D1 gene in prostate epithelial cells in vitro and in vivo. Cancer Res 2007; 67:4364-72; PMID:17483350; DOI:10.1158/0008-5472.CAN-06-1898.